Inorganic Chemistry
Article

Inorg. Chem. 2010, 49, 4319–4323 4319
DOI: 10.1021/ic100308j

Stepwise Phase Transition in the Formation of Lithium Amidoborane

Chengzhang Wu,[†] Guotao Wu,[*,†] Zhitao Xiong,[†] William I. F. David,[‡,§] Kate R. Ryan,[‡,§] Martin O. Jones,[‡,§] Peter P. Edwards,[§] Hailiang Chu,[†] and Ping Chen[*,†]

[†]*Dalian Institute of Chemical Physics, Chinese Academy of Sciences, 457 Zhongshan Road, Dalian 116023, People's Republic of China,* [‡]*Rutherford Appleton Laboratory, Harwell Science and Innovation Campus, Didcot OX11 0QX, U.K., and* [§]*Department of Chemistry, ICL, University of Oxford, South Parks Road, Oxford OX1 2JD, U.K.*

Received February 14, 2010

A stepwise phase transition in the formation of lithium amidoborane via the solid-state reaction of lithium hydride and ammonia borane has been identified and investigated. Structural analyses reveal that a lithium amidoborane—ammonia borane complex ($LiNH_2BH_3 \cdot NH_3BH_3$) and two allotropes of lithium amidoborane (denoted as α- and β-$LiNH_2BH_3$, both of which adopt orthorhombic symmetry) were formed in the process of synthesis. $LiNH_2BH_3 \cdot NH_3BH_3$ is the intermediate of the synthesis and adopts a monoclinic structure that features layered $LiNH_2BH_3$ and NH_3BH_3 molecules and contains both ionic and dihydrogen bonds. Unlike α-$LiNH_2BH_3$, the units of the β phase have two distinct Li^+ and $[NH_2BH_3]^-$ environments. β-$LiNH_2BH_3$ can only be observed in energetic ball milling and transforms to α-$LiNH_2BH_3$ upon extended milling. Both allotropes of $LiNH_2BH_3$ exhibit similar thermal decomposition behavior, with 10.8 wt % H_2 released when heated to 180 °C; in contrast, $LiNH_2BH_3 \cdot NH_3BH_3$ releases approximately 14.3 wt % H_2 under the same conditions.

Introduction

The development of a viable hydrogen-storage system for fuel-cell vehicles is of significant importance in the transition from a carbon-based to a hydrogen-based economy. Recent research on materials design and synthesis has mainly focused on chemicals that are composed of light elements and possess high hydrogen content.[1] One significant material that has been investigated is ammonia borane, NH_3BH_3, a solid-state compound with 19.6 wt % hydrogen capacity. Ammonia borane was first synthesized in 1955,[2] and its room-temperature body-centered tetragonal structure was determined in the subsequent year.[3] Hoon and Reynhardt[4] observed a phase transition from a tetragonal to an orthorhombic structure at low temperatures. Subsequently, Klooster et al.,[5] Bowden et al.,[6] and Hess et al.[7] confirmed this orthorhombic structure using neutron diffraction, single-crystal X-ray diffraction (XRD), and in situ Raman, respectively. NH_3BH_3 decomposes to hydrogen upon heating,[8] and its application as a hydrogen-storage material was investigated by Wolf et al.[9a] and Gutowska et al.[9b] In the past decade, considerable attention has been given to NH_3BH_3 to improve its dehydrogenation properties.[9] More recently, there have been significant efforts to chemically modify ammonia borane through substitution of one of the protic hydrogen atoms with an alkali or alkaline-earth element.[10–13] Xiong et al. reported that lithium amidoborane, $LiNH_2BH_3$, could be synthesized

---

*To whom correspondence should be addressed. E-mail: pchen@dicp.ac.cn (P.C.), wgt@dicp.ac.cn (G.W.).

(1) (a) Orimo, S. I.; Nakamori, Y.; Eliseo, J. R.; Zuttel, A.; Jensen, C. M. *Chem. Rev.* **2007**, *107*, 4111–4132. (b) Chen, P.; Xiong, Z. T.; Luo, J. Z.; Lin, J. Y.; Tan, K. L. *Nature* **2002**, *420*, 302–304.

(2) Shore, S. G.; Parry, R. W. *J. Am. Chem. Soc.* **1955**, *77*, 6084–6085.

(3) (a) Hughes, E. W. *J. Am. Chem. Soc.* **1956**, *78*, 502–503. (b) Lippert, E. L.; Lipscomb, W. N. *J. Am. Chem. Soc.* **1956**, *78*, 503–504.

(4) Hoon, C. F.; Reynhardt, E. C. *J. Phys. C* **1983**, *16*, 6129–6136.

(5) Klooster, W. T.; Koetzle, T. F.; Siegbahn, P. E. M.; Richardson, T. B.; Crabtree, R. H. *J. Am. Chem. Soc.* **1999**, *121*, 6337–6343.

(6) Bowden, M. E.; Gainsford, G. J.; Robinson, W. T. *Aust. J. Chem.* **2007**, *60*, 149–153.

(7) Hess, N. J.; Bowden, M. E.; Parvanov, V. M.; Mundy, C.; Kathmann, S. M.; Schenter, G. K.; Autrey, T. *J. Chem. Phys.* **2008**, 128.

(8) Hu, M. G.; Geanangel, R. A.; Wendlandt, W. W. *Thermochim. Acta* **1978**, *23*, 249–255.

(9) (a) Wolf, G.; Baumann, J.; Baitalow, F.; Hoffmann, F. P. *Thermochim. Acta* **2000**, *343*, 19–25. (b) Gutowska, A.; Li, L. Y.; Shin, Y. S.; Wang, C. M. M.; Li, X. H. S.; Linehan, J. C.; Smith, R. S.; Kay, B. D.; Schmid, B.; Shaw, W.; Gutowski, M.; Autrey, T. *Angew. Chem., Int. Ed.* **2005**, *44*, 3578–3582. (c) Chandra, M.; Xu, Q. *J. Power Sources* **2006**, *156*, 190–194. (d) Stowe, A. C.; Shaw, W. J.; Linehan, J. C.; Schmid, B.; Autrey, T. *Phys. Chem. Chem. Phys.* **2007**, *9*, 1831–1836. (e) Heldebrant, D. J.; Karkamkar, A.; Hess, N. J.; Bowden, M.; Rassat, S.; Zheng, F.; Rappe, K.; Autrey, T. *Chem. Mater.* **2008**, *20*, 5332–5336. (f) He, T.; Xiong, Z. T.; Wu, G. T.; Chu, H. L.; Wu, C. Z.; Zhang, T.; Chen, P. *Chem. Mater.* **2009**, *21*, 2315–2318.

(10) Xiong, Z. T.; Yong, C. K.; Wu, G. T.; Chen, P.; Shaw, W.; Karkamkar, A.; Autrey, T.; Jones, M. O.; Johnson, S. R.; Edwards, P. P.; David, W. I. F. *Nat. Mater.* **2008**, *7*, 138–141.

(11) Diyabalanage, H. V. K.; Shrestha, R. P.; Semelsberger, T. A.; Scott, B. L.; Bowden, M. E.; Davis, B. L.; Burrell, A. K. *Angew. Chem., Int. Ed.* **2007**, *46*, 8995–8997.

(12) Kang, X. D.; Fang, Z. Z.; Kong, L. Y.; Cheng, H. M.; Yao, X. D.; Lu, G. Q.; Wang, P. *Adv. Mater.* **2008**, *20*, 2756.

(13) Wu, H.; Zhou, W.; Yildirim, T. *J. Am. Chem. Soc.* **2008**, *130*, 14834–14839.

from the direct reaction of LiH with NH_3BH_3.

$$LiH + NH_3BH_3 \rightarrow LiNH_2BH_3 + H_2 \qquad (1)$$

One of the driving forces suggested for the formation of $LiNH_2BH_3$ is the high chemical potential for the combination of the protic $H^{\delta+}$ in NH_3 with the hydridic $H^{\delta-}$ in alkali-metal hydrides to form H_2. $LiNH_2BH_3$ crystallizes in the orthorhombic space group *Pbca*, with $a = 7.11274(6)$ Å, $b = 13.94877(14)$ Å, $c = 5.15018(6)$ Å, and $V = 510.970(15)$ Å^3, which is consistent with Wu et al.'s results.[13] $LiNH_2BH_3$ releases 10.9 wt % of hydrogen without borazine formation at 91 °C.[10] The systematic first-principles study of the structural and energetic properties of $LiNH_2BH_3$ by Ramzan et al. is in agreement with the experimental data.[14] The mechanism of dehydrogenation was modeled by Kim et al.[15] More recently, a new allotrope of $LiNH_2BH_3$ was synthesized that also crystallizes in space group *Pbca* but with different lattice constants: $a = 15.146(6)$ Å, $b = 7.721(3)$ Å, $c = 9.268(4)$ Å, and $V = 1083.7(8)$ Å^3. This new allotrope is denoted as β-$LiNH_2BH_3$ to distinguish it from the originally discovered form of $LiNH_2BH_3$ (henceforth denoted as α-$LiNH_2BH_3$) reported by Xiong et al.[10] The derived space group implies an asymmetric unit with a volume of 135.5(1) Å^3 that is essentially twice the volume of α-$LiNH_2BH_3$ (63.8 Å^3), implying that there are two crystallographically distinct Li and NH_2BH_3 ions.

The formation of $LiNH_2BH_3$ via a solution-based route, i.e., by using tetrahydrofuran (THF) as a solvent, was monitored recently by in situ NMR.[16] A gradual shift in the resonance of ^{11}B was observed, which indicated that the formation of $LiNH_2BH_3$ was a stepwise process. Therefore, it is of significant importance to characterize the compositionally induced structural changes obtained when using a conventional solid-state synthesis. In this study, we systematically investigated the formation of $LiNH_2BH_3$ via the mechanical milling of molar equivalents of LiH and NH_3BH_3. Our experimental results show that the amidoborane–ammonia borane complex is formed at the initial stage of the reaction and is subsequently converted to $LiNH_2BH_3$, with two phases of $LiNH_2BH_3$, namely, α-$LiNH_2BH_3$ and β-$LiNH_2BH_3$, identified in the process. Interestingly, both phases of lithium amidoborane exhibit essentially identical features in dehydrogenation.

Experimental Section

Synthesis. Lithium hydride (LiH, 99%, Aldrich) and ammonia borane (NH_3BH_3, 98%, Aldrich) in a molar ratio of 1:1 were mechanically milled together under 1 bar of argon at 200 rpm on a planetary mill (Retsch, PM400). The extent of reaction was monitored by recording the pressure change in the milling vial. The content of the gaseous product(s) was analyzed by mass spectrometry (Hiden HPR-20 Gas Analysis System) and a thermoconductivity meter (accuracy, 0.1 μs/cm), where the outlet gas was introduced to a dilute H_2SO_4 solution whose ion conductivity was monitored with the progression of dehydrogenation. It should be noted that the ionic conductivity of the solution will decrease if NH_3 is released from the sample and absorbed by the solution. The synthesis process was stopped at different stages for sample collection.

Dehydrogenation. A homemade temperature-programmed desorption–mass spectrometry (Hiden HPR-20) combined system was employed to detect the gaseous products evolved in the thermal decomposition processes. Volumetric release for quantitative measurements of hydrogen desorption from samples was performed on a HyEnergy PCT apparatus. The heat flow in the thermal dehydrogenation was also monitored by a Netzch 449C thermogravimetric/differential scanning calorimetry (TG/DSC) unit. The ammonia concentration in the gaseous phase was measured from solution thermoconductivity.

Characterization. Structural identification was undertaken on a PANalytical X'pert diffractometer (Cu KR, 40 kV, 40 mA) and also on the high-resolution diffractometers ID31 at the European Synchrotron Radiation Facility, Grenoble, France, at a wavelength of 0.79825(1) Å and BL14B1 at the Shanghai Synchrotron Radiation Facility, Shanghai, China, at a wavelength of 1.2398 Å.

Results and Discussion

Phase Transition in the Formation of Lithium Amidoborane. To explore the formation mechanism of lithium amidoborane, a 1:1 molar ratio of LiH and NH_3BH_3 was mechanically milled, and the extent of reaction was monitored by recording the increase in the pressure in the milling vial as a function of the time. The gaseous products were analyzed by mass spectrometry and an ammonia detection device. The ammonia concentration was found to be less than 300 ppm upon completion of the reaction, and thus the majority of the gaseous product is H_2 (eq 1). The extent of reaction is correlated with the amount of H_2 generated. Solid residues collected at different stages of the reaction were subject to structural characterization. As shown in Figure 1, when approximately $^1/_3$ mol equiv of H_2 had evolved, the solid residue was composed of unreacted LiH and $LiNH_2BH_3 \cdot NH_3BH_3$, a new phase, recently identified by the authors, that can be obtained by the mechanical milling of a 1:2 molar ratio of LiH and NH_3BH_3 or a 1:1 molar ratio of $LiNH_2BH_3$ and NH_3BH_3.[17] It should be noted that the absence of unreacted NH_3BH_3 in the XRD pattern is likely due to the deformation of NH_3BH_3 into an amorphous phase under energetic ball milling. After ca. $^2/_3$ mol equiv of H_2 had evolved, α-$LiNH_2BH_3$ and $LiNH_2BH_3 \cdot NH_3BH_3$ were found to coexist in the solid residue. When ca. $^3/_4$ mol equiv of H_2 had evolved, both α-$LiNH_2BH_3$ and β-$LiNH_2BH_3$ phases were present in the residue. Upon the release of ca. 1.0 mol equiv of H_2, the only phase detected was β-$LiNH_2BH_3$. On the basis of the above observations and analyses, the following reaction steps are proposed for the formation of $LiNH_2BH_3$ from LiH and NH_3BH_3 (wherein AB, LiAB, and LiABAB are the abbreviations for NH_3BH_3, $LiNH_2BH_3$, and $LiNH_2BH_3 \cdot NH_3BH_3$, respectively):

$$\begin{aligned} &2LiH + 2AB \\ &\rightarrow LiH + LiABAB + H_2 \\ &\rightarrow 2LiAB + 2H_2 \qquad (2) \end{aligned}$$

---

(14) Ramzan, M.; Silvearv, F.; Blomqvist, A.; Scheicher, R. H.; Lebegue, S.; Ahuja, R. *Phys. Rev. B* **2009**, *79*.

(15) Kim, D. Y.; Singh, N. J.; Lee, H. M.; Kim, K. S. *Chem.—Eur. J.* **2009**, *15*, 5598–5604.

(16) Xiong, Z. T.; Chua, Y. S.; Wu, G. T.; Xu, W. L.; Chen, P.; Shaw, W.; Karkamkar, A.; Linehan, J.; Smurthwaite, T.; Autrey, T. *Chem. Commun.* **2008**, 5595–5597.

(17) Wu, C. Z.; Wu, G. T.; Han, X. W.; Xiong, Z. T.; Chu, H. L.; He, T.; Chen, P. *Chem. Mater.* **2010**, *22*, 3.

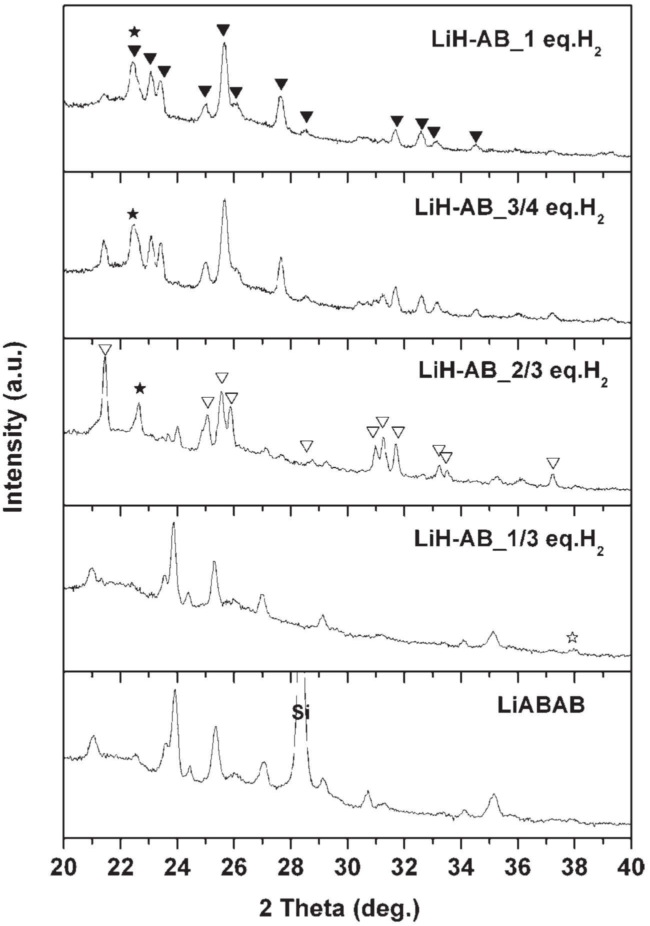

Figure 1. XRD patterns of LiH−NH_3BH_3 samples ball-milled for various times. The XRD pattern of $LiNH_2BH_3 \cdot NH_3BH_3$ is also presented for comparison (▽, α-$LiNH_2BH_3$; ▼, β-$LiNH_2BH_3$; ★, post-decomposed product of $LiNH_2BH_3 \cdot NH_3BH_3$; ☆, LiH). The diffraction peak at $2\theta = 22.7°$ is the product of the decomposition of $LiNH_2BH_3 \cdot NH_3BH_3$.[17].

We have examined the interaction of $LiNH_2BH_3 \cdot NH_3BH_3$ synthesized separately[17] with 1.0 mol equiv of LiH to confirm the second step in the process described above, i.e., that the formation of $LiNH_2BH_3$ is the result of a further substitution of H by Li in $LiNH_2BH_3 \cdot NH_3BH_3$. Our results show that β-$LiNH_2BH_3$ is formed, after the addition of ca. 1.0 mol equiv of H_2, from the reaction of $LiNH_2BH_3 \cdot NH_3BH_3$ with LiH. Interestingly, increasing the LiH content for the reaction of $LiNH_2BH_3 \cdot NH_3BH_3$ with LiH did not lead to a further substitution of H by Li; i.e., there is no evidence for the formation of speculated species "Li_2NHBH_3".[18]

It should be noted that a tetragonal phase with a unit cell of $a = 4.0320(4)$ Å, $c = 17.023(4)$ Å, and $V = 276.73(8)$ Å^3 was present in most of the samples. This phase likely originated from the dehydrogenation/decomposition of $LiNH_2BH_3 \cdot NH_3BH_3$.[17]

It is interesting to note that $LiNH_2BH_3$ initially formed is of the α phase, which then transforms to the β phase as the reaction progresses. Moreover, we noted that β-$LiNH_2BH_3$ subsequently transformed back to α-$LiNH_2BH_3$ upon extended ball milling. As shown in Figure 2, β-$LiNH_2BH_3$ gradually converted to α-$LiNH_2BH_3$ upon mechanical milling at 200 rpm for 16 h. It should be noted that no pressure change was detected in such a transformation, which suggests that the chemical composition of the solid remains unchanged.

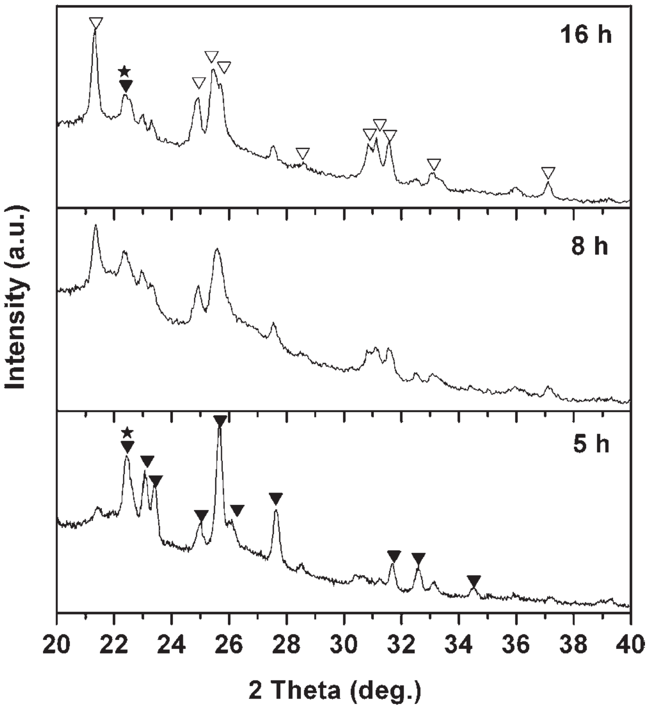

Figure 2. XRD patterns of LiH−NH_3BH_3 ball-milled for 5, 8, and 16 h, respectively. β-$LiNH_2BH_3$ tends to transform to α-$LiNH_2BH_3$ through extended milling (▽, α-$LiNH_2BH_3$; ▼, β-$LiNH_2BH_3$; ★, postdecomposed product of $LiNH_2BH_3 \cdot NH_3BH_3$).

Structural information for $LiNH_2BH_3 \cdot NH_3BH_3$ and α- and β-$LiNH_2BH_3$ is presented in Table 1. It can be seen that the lattice parameters of $LiNH_2BH_3 \cdot NH_3BH_3$ are close to those of α-$LiNH_2BH_3$ but approximately half of those of β-$LiNH_2BH_3$. The coordination environments of Li^+ in α-$LiNH_2BH_3$, β-$LiNH_2BH_3$, and $LiNH_2BH_3 \cdot NH_3BH_3$ are presented in Figure 3. The strongest interaction in all of the structures is the ionic bond formed between the Li^+ cation and nitrogen atom in the amidoborane anion and $H^{\delta-}$ in the BH_3 group. As shown in Figure 3a, the Li−N bond length in α-$LiNH_2BH_3$ is 2.02 Å; each Li^+ is surrounded by three BH_3 groups of $[NH_2BH_3]^-$ ions with Li−B distances in the range of 2.64− 2.68 Å. The crystal structure of β-$LiNH_2BH_3$ is an intergrowth of two different $LiNH_2BH_3$ layers oriented perpendicular to the *a* axis, and here the bond lengths for Li_1−N and Li_2−N are 1.93 and 2.04 Å, respectively. Moreover, the tetrahedral coordination of Li^+ ions in β-$LiNH_2BH_3$ is distorted: the Li_1−B distances are 2.56, 2.57, and 2.78 Å, respectively. However, the Li_2−B distances are 2.50, 2.51, and 2.92 Å (Figure 3b), respectively. For the intermediate $LiNH_2BH_3 \cdot NH_3BH_3$, each Li^+ bonds with one $[NH_2BH_3]^-$ ion (Li−N distance 2.05 Å) and is also coordinated with one BH_3 group of NH_3BH_3 and two BH_3 groups of $[NH_2BH_3]^-$ ions with Li−B distances of 2.48−2.58 Å (Figure 3c).

The symmetry of β-$LiNH_2BH_3$ is lower than that of α-$LiNH_2BH_3$ and could suggest that it is a metastable phase that arises as a result of the energetic mechanical

---

(18) Armstrong, D. R.; Perkins, P. G.; Walker, G. T. *THEOCHEM* **1985**, *23*, 189–203.

Table 1. Lattice Parameters of $LiNH_2BH_3 \cdot NH_3BH_3$, α-$LiNH_2BH_3$, and β-$LiNH_2BH_3$

			lattice parameters				
	crystal structure	space group	a (Å)	b (Å)	c (Å)	β (deg)	V (Å^3)
$LiNH_2BH_3 \cdot NH_3BH_3$[17]	monoclinic	$P2_1/c$	7.05	14.81	5.13	97.5	531.6
α−$LiNH_2BH_3$[10]	orthorhombic	*Pbca*	7.11	13.95	5.15	90.0	511.0
β−$LiNH_2BH_3$	orthorhombic	*Pbca*	15.15	7.72	9.27	90.0	1083.7

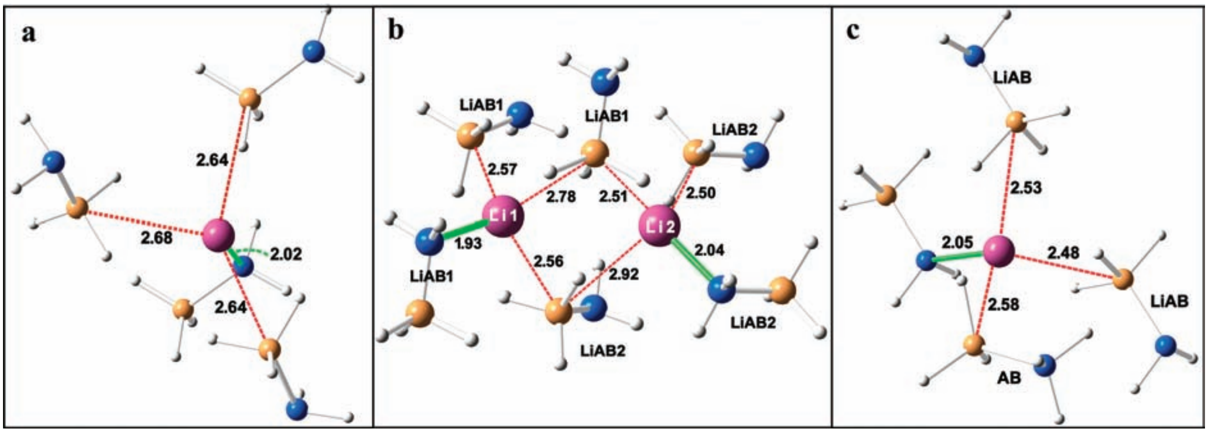

Figure 3. Tetrahedral coordination of Li^+ ions around amidoborane anions for (a) α-$LiNH_2BH_3$, (b) β-$LiNH_2BH_3$, and (c) $LiNH_2BH_3 \cdot NH_3BH_3$.

milling synthesis process. There are numerous cases where nonequilibrium phase transitions in solid materials occur under mechanical milling conditions,[19] for example, the metastable γ-MgH_2 phase (high-pressure phase) is formed upon the milling of stable β-MgH_2.[20] To date, β-$LiNH_2BH_3$ has only been obtained via mechanical milling synthesis.[16] Dissolving β-$LiNH_2BH_3$ in THF and then recrystallizing results in the formation of α-$LiNH_2BH_3$ (as characterized by XRD), which suggests that β-$LiNH_2BH_3$ may be kinetically stabilized and that α-$LiNH_2BH_3$ is the more thermodynamically stable species. This is supported by the fact that β-$LiNH_2BH_3$ transforms to α-$LiNH_2BH_3$ upon extended ball milling. Although the detailed mechanism for this phase transition is the subject of further study, the extended ball milling could lead to the regain of the equilibrium (thermodynamically stable) state.

Dehydrogenation Properties. Thermal decomposition properties of $LiNH_2BH_3 \cdot NH_3BH_3$, β-$LiNH_2BH_3$, and α-$LiNH_2BH_3$ were investigated on a PCT apparatus at 91 and 180 °C, respectively. As shown in Figure 4, β-$LiNH_2BH_3$ and α-$LiNH_2BH$ exhibit essentially identical dehydrogenation features; i.e., both release 8.8 wt % H_2 at 91 °C (ca. 1.6 mol equiv of H_2. Note that H_2 desorption is less than what we reported previously, which is due to the addition of carbon to the $LiNH_2BH_3$ sample[10]). Upon further heating to 180 °C, ca. 2.0 mol equiv of H_2 was released [see reaction (3)]. To further verify the similarity of the thermal decomposition of these two $LiNH_2BH_3$ phases, DSC measurements were also performed. Our results show that both α- and β-$LiNH_2BH_3$ exhibit an endothermic feature (starting from 82 °C) prior to the exothermic dehydrogenation, which is likely due to the melting of the material. The structural difference will, therefore, vanish under such a condition. The dehydrogenation should mainly reflect the chemical nature of the “molten” LiAB species.

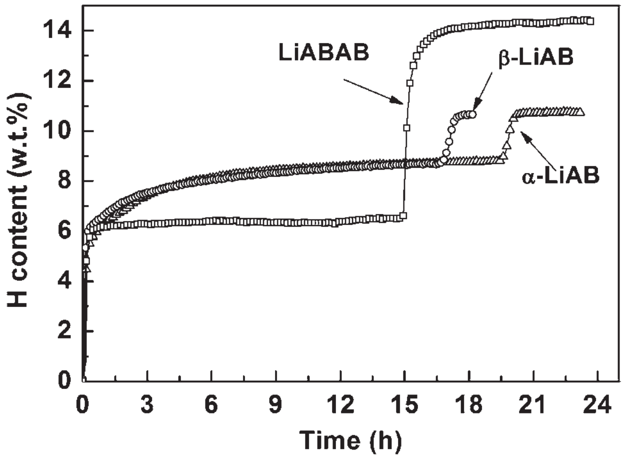

Figure 4. Time dependence of hydrogen release from $LiNH_2BH_3 \cdot NH_3BH_3$, α-$LiNH_2BH_3$, and β-$LiNH_2BH_3$ at two temperature stages, 91 and 180 °C, respectively. (Please note that the time−temperature profile for each sample is different.) For lithium amidoboranes, about 8.8 wt % H_2 released at 91 °C (close to 20 h, ca. 1.6 mol equiv of H_2) and a total of 2.0 mol equiv of H_2 released (10.8 wt %) during heating up to 180 °C. For $LiNH_2BH_3 \cdot NH_3BH_3$, first 6 wt % H_2 released at 91 °C and 8.3 wt % H_2 released at 180 °C. (The ammonia concentrations after thermal decomposition are ~300 ppm for α-$LiNH_2BH_3$ and β-$LiNH_2BH_3$ and less than 3000 ppm for $LiNH_2BH_3 \cdot NH_3BH_3$.)

$LiNH_2BH_3 \cdot NH_3BH_3$ prepared by directly milling a 1:2 molar ratio of LiH/NH_3BH_3 was observed to release 6.0 wt % (ca. ~2 mol equiv) H_2 at 91 °C and 8.3 wt % (ca. ~3 mol equiv) H_2 at 180 °C, a total of 14.3 wt % H_2, which is close to its theoretical capacity of 14.8 wt % [see reaction (4)].[17]

$$n\mathrm{LiNH_2BH_3(s)} \rightarrow \mathrm{(LiNBH)}_n\mathrm{(s)} + 2n\mathrm{H_2(g)} \qquad (3)$$

$$n\mathrm{LiNH_2BH_3 \cdot NH_3BH_3(s)} \rightarrow \mathrm{(LiN_2B_2H)}_n\mathrm{(s)} + 5n\mathrm{H_2(g)} \qquad (4)$$

---

(19) Suryanarayana, C. *Prog. Mater. Sci.* **2001**, *46*, 1–184.

(20) Varin, R. A.; Czujko, T.; Wronski, Z. *Nanotechnology* **2006**, *17*, 3856–3865.

Conclusion

In summary, $LiNH_2BH_3 \cdot NH_3BH_3$ and α and β phases of $LiNH_2BH_3$ were observed as products of the solid-state reaction of LiH and NH_3BH_3. The $LiNH_2BH_3 \cdot NH_3BH_3$ complex, possessing a monoclinic structure and composed of alternative $LiNH_2BH_3$ and NH_3BH_3 layers, is the intermediate phase in the formation of $LiNH_2BH_3$. β-$LiNH_2BH_3$, a metastable phase formed under mechanical milling conditions, converts back to α-$LiNH_2BH_3$ upon either extended ball milling or recrystallization from THF. Both polymorphs of lithium amidoborane (α- and β-$LiNH_2BH_3$) release approximately 10.8 wt % H_2 upon heating to 180 °C, whereas $LiNH_2BH_3 \cdot NH_3BH_3$ releases approximately 14.3 wt % H_2 under the same conditions.

Acknowledgment. The authors acknowledge financial support from the Hundred Talents Project and Knowledge Innovation Program of CAS (Grants KGCX2-YW-806 and KJCX2-YW-H21), National Program on Key Basic Research Project (973 Program, No. 2010CB631304), and National High-tech R&D Program of China (863 Program, No. 2009AA05Z108). We further acknowledge support of the EPSRC funding bodies and the United Kingdom Sustainable Hydrogen Energy Consortium (UK-SHEC), an EPSRC SUPERGEN.